LASER INTERFEROMETER GRAVITATIONAL WAVE OBSERVATORY
- LIGO -
CALIFORNIA INSTITUTE OF TECHNOLOGY
MASSACHUSETTS INSTITUTE OF TECHNOLOGY

Technical Note	LIGO-T1300354-v3	July 30, 2013

Scattered light noise due to the ETM coating ripple

P. Fritschel, H. Yamamoto

California Institute of Technology
LIGO Project, MS 18-34
Pasadena, CA 91125
Phone (626) 395-2129
Fax (626) 304-9834
E-mail: info@ligo.caltech.edu

Massachusetts Institute of Technology
LIGO Project, Room NW22-295
Cambridge, MA 02139
Phone (617) 253-4824
Fax (617) 253-7014
E-mail: info@ligo.mit.edu

LIGO Hanford Observatory
Route 10, Mile Marker 2
Richland, WA 99352
Phone (509) 372-8106
Fax (509) 372-8137
E-mail: info@ligo.caltech.edu

LIGO Livingston Observatory
19100 LIGO Lane
Livingston, LA 70754
Phone (225) 686-3100
Fax (225) 686-7189
E-mail: info@ligo.caltech.edu

http://www.ligo.caltech.edu/

1 Introduction

This note contains an estimate of the noise due to the scattered light ring pattern from the ETM, arising from the periodic thickness variations produced by the LMA double-planetary coating process.[1] The phenomenon analyzed is where this scattered light ring hits a beam tube baffle near the ITM end of the tube, is scattered back towards the ETM by the baffle material, and then scatters back into the cavity mode on the ETM surface. Vibrations of the baffle will phase modulate this recombined light, producing phase noise on the cavity beam. While some parts of the scattered light ring will hit the arm cavity baffle and the manifold/cryopump baffle, both of these baffles have some amount of vibration isolation, so the phase noise from these scattering paths should be small compared to the beam tube baffle case.

2 Executive summary

The noise estimate is shown in Figs. 10 and 11 at the end of this note. There is a considerable range of estimates, due to differences in the various measurements of beam tube vibrations. A 13-14 Hz mode of the beam tube can encroach on the target strain sensitivity, possibly exceeding it by a factor of several, and certainly exceeding the technical noise limit. More measurements of the beam tube vibrations should be made–at LLO as well as LHO–to get a more complete picture. However, in any case a solution to the coating thickness ripple should be explored with LMA. A final note is that any excess scattered light noise from this source should be confined to frequencies below 30 Hz, and as such would have minimal impact on sensitivity to binary neutron star inspirals.

3 Scattered light cone

3.1 Coating ripple

The high-reflectivity coatings applied by LMA on ETM07 and ETM09 show a distinct azimuthal ripple in the coating surface height (coating thickness), at radii beyond about 3 cm from the mirror center. The maximum amplitude of the ripple is about 1 nm pk-pk at a radius of 4 cm, and the spatial wavelength of the (near-sinusoidal) ripple is 7.85 mm. Since the ripple does not extend to the center of the mirror, it does not produce much loss: 6 ppm is diffracted out of the main beam due to the ripple. More details of the coating ripple can be found in LIGO-T1300183.

3.2 Diffraction cone properties

The coating ripple produces a diffraction cone, with a half-angle of $\theta_r = \lambda/7.85$ mm $= 1.36 \times 10^{-6}$ rad. The angular width of the cone is about $\Delta\theta_r = 2 \times 10^{-5}$. Most of this

[1] This note contains much of the same information found in T1300323, but the contents and results of this note supersede T1300323.

scattered light hits the beam tube baffles, although since the cavity axis is offset with respect to the beam tube axis, some of it hits the manifold/cryo baffle and arm cavity baffle (both at the ITM end). Figure 1 shows the geometry of the diffraction cone with respect to the beam tube and baffles.

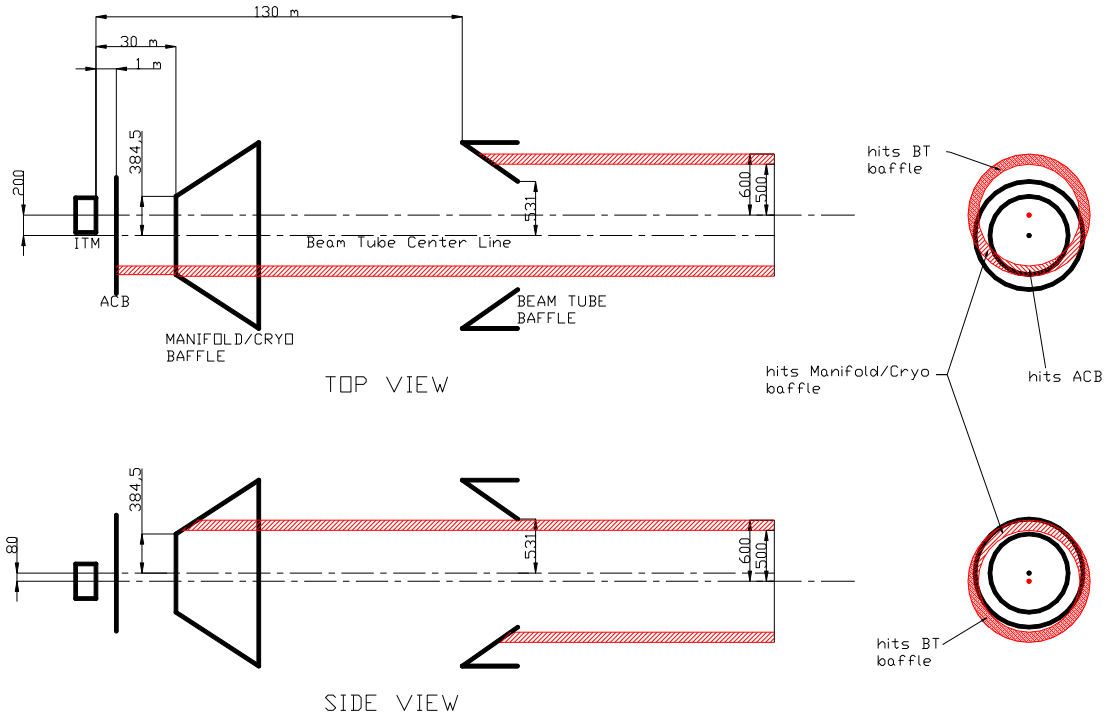

Figure 1: Geometry of the scattered light ring, the beam tube, and the three types of baffles. Drawing courtesy of Mike Smith.

The scattered light from the ETM coating has been calculated using the SIS (Stationary Interferometer Simulation) to simulate an arm cavity using the ETM07 phase maps and an ideal ITM. Figure 2 shows the power distribution at the plane of the ITM, both for the full plane and with apertures appropriate to the different baffles. The radial power distribution from the beam axis is shown in Fig. 3, calculated as:

$$\begin{aligned} P(r) &= \int_0^{2\pi} d\phi \cdot P(r,\phi) \\ P_{out}(r) &= \int_r^{\infty} dr' \cdot P(r') \,, \end{aligned}$$

where $P_{out}(r)$ is the total power outside of the radius r.

Figure 4 shows the radial power distribution at several distances from the ETM, and Fig. 5 shows the power distribution on a baffle 3 km from the ETM.

4 Backscatter noise calculation

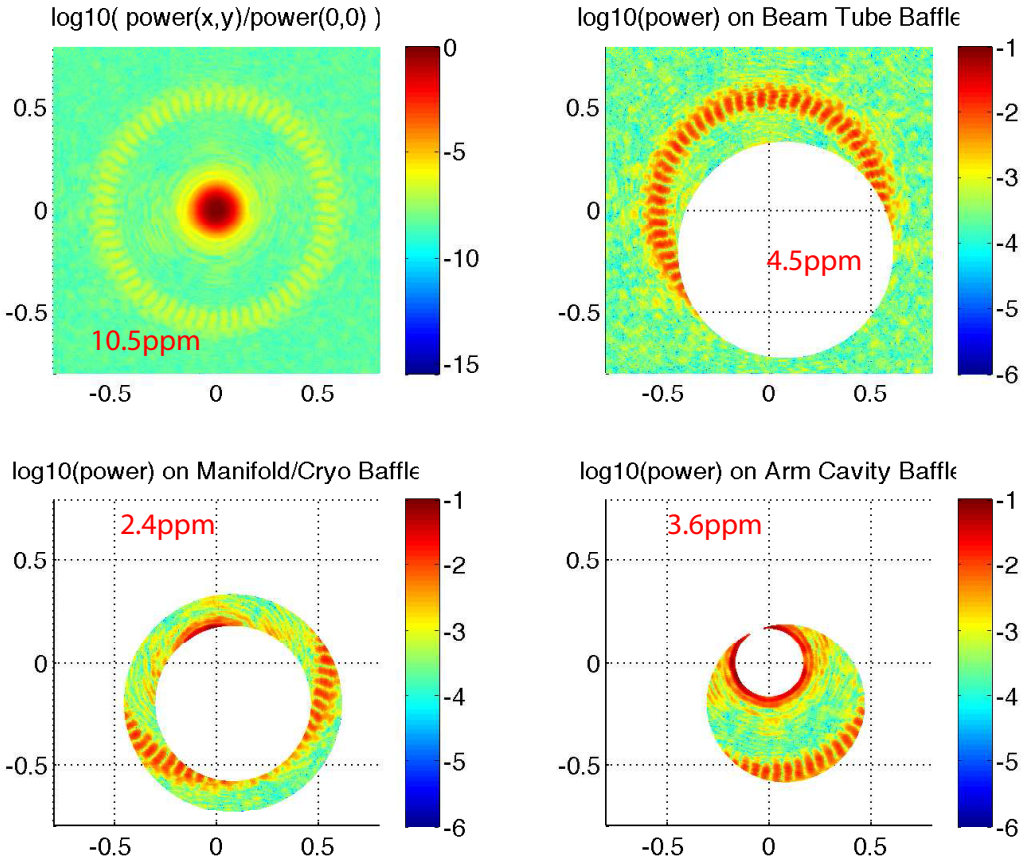

Figure 2: Power distribution in the plane of the ITM, from the SIS output. The axes are in meters, and the cavity axis is at the origin. The cavity axis is offset from the beam tube axis by 20 cm horizontally, and by 8 cm vertically (cavity axis below the BT center); note that horizontal and vertical in the plots do not correspond to their physical counterparts (turn the page 90 deg CW if you care). Upper left panel: entire power distribution; the spot near the center is the main cavity beam. Total power outside the main beam is 10.5 ppm, of which 6 ppm is in the diffraction ring. Upper right: power outside the aperture determined by the beam tube baffle at 4 km; total scattered power in this area is 4.5 ppm. Lower left: power on the manifold/cryo baffle annulus; total scattered power 2.4 ppm. Lower right: Power on the arm cavity baffle; total scattered power 3.6 ppm.

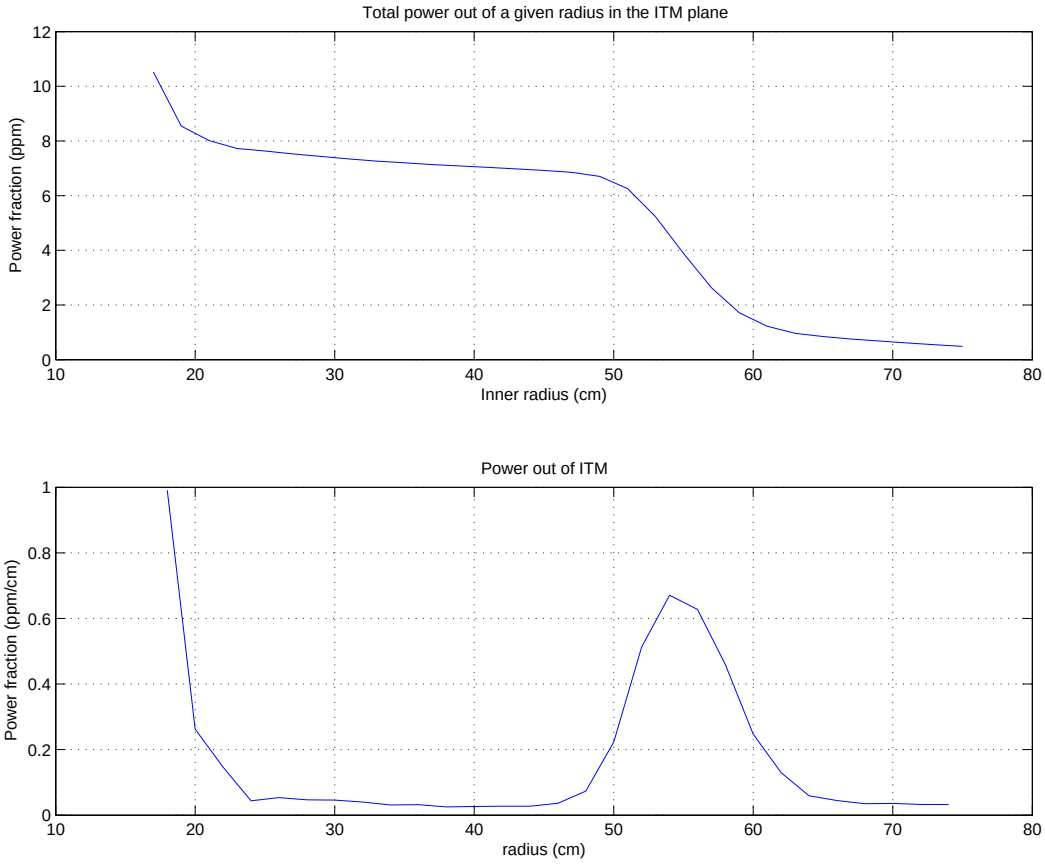

Figure 3: Radial power distribution in the plane of the ITM. Lower panel is $P(r)$ and upper panel is $P_{out}(r)$. The latter shows that the total power in the ring is 6 ppm.

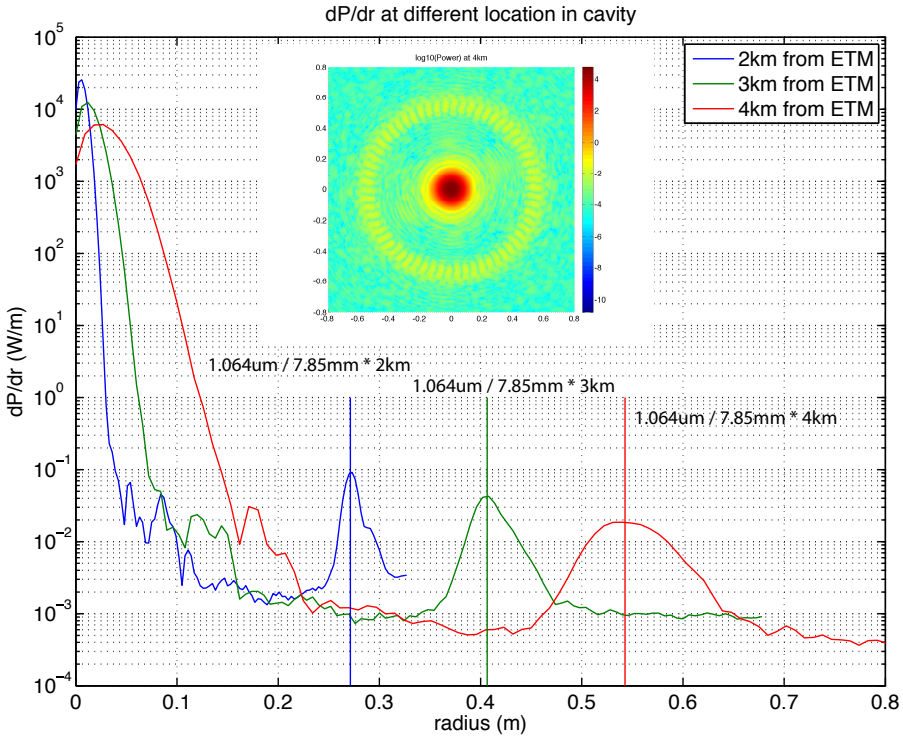

Figure 4: Radial power distribution at three points along the cavity axis. The diffraction ring peaks at a radius determined by the diffraction cone angle. The width of the diffraction ring is equal to the cavity mode beam diameter: 2.4 cm at 2 km and 10.6 cm at 4 km.

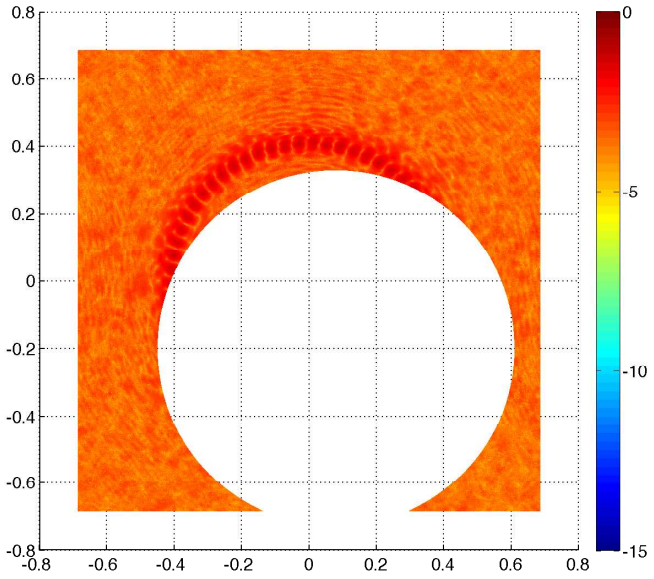

Figure 5: Power distribution in the plane 3 km from the ETM. The axes are in meters, and the cavity axis is at the origin.

4.1 Method

The analysis follows the methods of Flanagan and Thorne in LIGO-T940063, *Noise Due to Backscatter Off Baffles, the Nearby Wall, and Objects at the Far end of the Beam Tube*. Simply put, the equivalent test mass displacement noise is equal to the scatterer (baffle) displacement noise, scaled by the ratio of the scattered light field to the main beam field, both in the arm cavity mode:

$$\delta\tilde{x}^2_{TM}(f) = \frac{1}{2}\,\frac{\delta I_{mb}}{I_{mb}}\,\tilde{x}^2_b(f) \tag{1}$$

Here I_{mb} is the arm cavity power in the main beam, δI_{mb} is the scattered light power that has been recombined into the cavity main beam, and x_b is the motion of the beam tube baffle, along the direction parallel to the incoming and backscattered light rays (so, essentially along the beam tube axis). The factor of 1/2 comes from the fact that 1/2 of the baffle motion, in power, is in the phase quadrature of the main field. The above formula is a combination of equations 12 and 28 in T940063.

To find the recombined scattered light power, use equation 17 of T940063:

$$\frac{\delta I_{mb}}{I_{mb}} = \frac{\lambda^2}{r^2}\left(\frac{dP}{d\Omega_{ms}}\right)^2 \frac{dP}{d\Omega_{bs}}\delta\Omega_{ms} \tag{2}$$

This is the power scattered back into the main beam from the small solid angle $\delta\Omega_{ms}$, given

the mirror's probability $dP/d\Omega_{ms}$ to scatter main-beam photons into a unit solid angle in the direction of $\delta\Omega_{ms}$, and the probability $dP/d\Omega_{bs}$ for a photon arriving at the backscatter surface (baffle) to get backscattered into a unit solid angle in the direction of the mirror, and the distance r between the mirror and the location of backscatter. The key feature of this expression is the use of a reciprocity relation, derived in T940063, that links the mirror's probability to scatter light out of the main beam and into a certain direction, and the cross section (σ_{ms}) for that same mirror to scatter an incoming light flux from that same direction back into the main beam. That relation is:

$$\sigma_{ms} = \lambda^2 \frac{dP}{d\Omega_{ms}} \,.$$

4.2 Simplified analysis for a single baffle

We start with a simplified analysis for a single beam tube baffle that intercepts the scattered light ring as shown in Fig. 3. In this case the small solid angle $\delta\Omega_{ms}$ is that of the ring pattern:

$$\delta\Omega_{ms} = 2\pi\Delta\theta_r\theta_r = 1.7\times10^{-8}\,\mathrm{str}\,,$$

where $\theta_r = 1.36\times10^{-4}$ rad is the diffraction angle of the ring, and $\Delta\theta_r = 2\times10^{-5}$ rad is the angular width of the ring. This is actually a simplification, because the intensity in the ring pattern is not uniform around the ring. The azimuthal ripple will decrease the effective solid angle.

The total fractional power scattered into the ring, from one ETM, is 6 ppm. This gives us the factor $(dP/d\Omega_{ms})\delta\Omega_{ms} = 6\times10^{-6}$. We also need just the factor $dP/d\Omega_{ms}$, which can be calculated from the preceding:

$$dP/d\Omega_{ms} = 6\times10^{-6}/1.7\times10^{-8}\mathrm{str} = 350/\mathrm{str}$$

Again, this is a simplification for a uniform intensity scattered light ring.

For a single baffle at a distance r from the ETM, the equivalent test mass noise is:

$$\begin{aligned}
\delta\tilde{x}^2_{TM}(f) &= \frac{1}{2}\left(\frac{\lambda}{r}\right)^2 \left[\frac{dP}{d\Omega_{ms}}\delta\Omega_{ms}\right]\frac{dP}{d\Omega_{ms}}\frac{dP}{d\Omega_{bs}}\,\tilde{x}^2_b(f) \\
&= 3.5\times10^{-20}\left(\frac{4000\mathrm{m}}{r}\right)^2\cdot[4.5\times10^{-6}]\cdot350\,\mathrm{str}^{-1}\cdot0.02\,\mathrm{str}^{-1}\cdot\tilde{x}^2_b(f) \\
\delta\tilde{x}_{TM}(f) &= 1.1\times10^{-12}\left(\frac{4000\mathrm{m}}{r}\right)\tilde{x}_b(f)
\end{aligned}$$

4.3 Summing over baffles

To account for the fact that the scattered light ring power hits and is re-scattered by many baffles, we compute the recombined scattered light power (equation 2) for each baffle that intercepts the ring, and add up the resulting powers to get the final recombined power. Rearranging terms of that equation, the recombined scattered light power from the i-th baffle is:

$$\frac{\delta I^i_{mb}}{I_{mb}} = \lambda^2 \frac{dP}{d\Omega_{bs}} \left[\frac{1}{r^2} \left(\frac{dP}{d\Omega_{ms}} \right)^2 \delta\Omega_{ms} \right]^i = \lambda^2 \frac{dP}{d\Omega_{bs}} K^i \tag{3}$$

The last factor (in square brackets) will be different for each baffle segment. Since the scattered light hitting each baffle is not necessarily of uniform intensity, it must be calculated by integrating the power distribution on each baffle. Figure 6 shows how a baffle intercepts the scattered light, for two baffle locations.

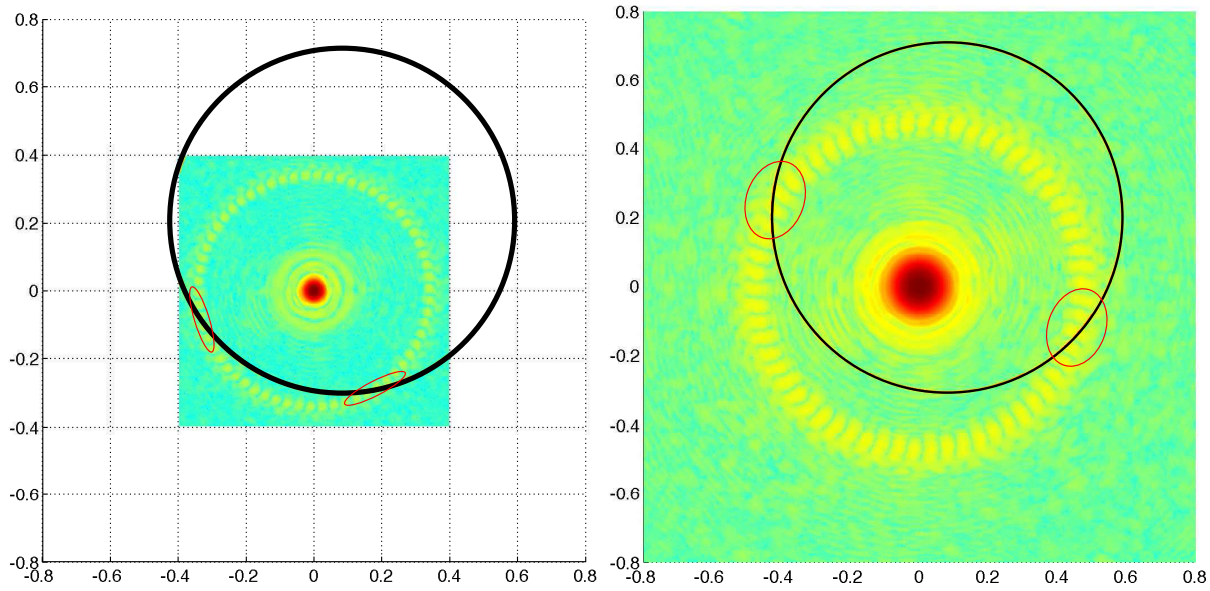

Figure 6: Power distribution in a 80 cm^2 plane. Left: 2500 m from the ETM. Right: 3500 m from the ETM. The black circle is the unshadowed ring of the baffle at that location. The red ovals indicate the portions of these baffles that receive some of the diffraction ring power.

For this analysis, the baffle locations for the LIGO-Livingston beam tube are used, as documented in LIGO-E950083-B. There are 108 baffles in each 2 km beam tube section. The baffle locations, spacing, and the visible ring width of each baffle are shown in Fig. 7. The scattered light power hitting each baffle, calculated using the SIS output, is shown in Fig. 8. Summing over baffles gives the result:

$$\sum_i K^i = 1.9 \times 10^{-10}\,\mathrm{m}^2\,. \tag{4}$$

We note that this sum gives a total power on the baffles of 3.5 ppm, about 20% smaller than the 4.5 ppm given in Fig. 2; the difference is due to power in the outer regions of the Fig. 2 plane that is not counted here, but does not contribute significantly to ΣK^i.

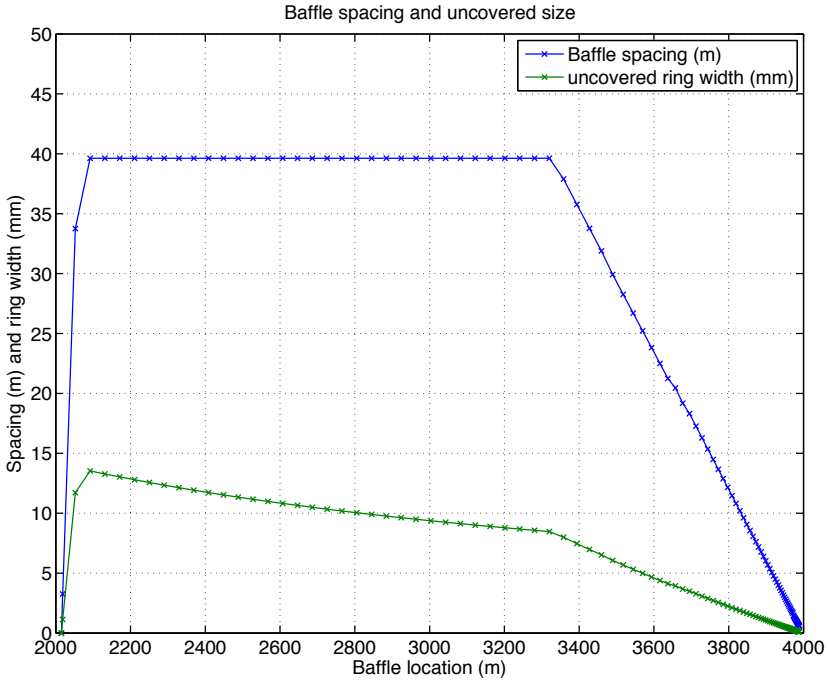

Figure 7: Markers (blue) indicate baffle locations and spacing between baffles, for LLO, from E950083-B. Green markers indicate the width of the baffle ring, as visible from the ETM.

4.4 Including radiation pressure

The treatment in T940063 does not include radiation pressure from scattered light; it considers only the component of the scattered light that changes the phase of the cavity beam. To include the radiation pressure effect, we must also calculate the cavity field amplitude fluctuations, then the radiation force and resulting test mass position fluctuations. To do that we back up a bit; start with equation 9 of T940063:

$$\frac{\delta\psi_{mb}}{\psi_{mb}} = \left(\frac{\delta I_{mb}}{I_{mb}}\right)^{1/2} e^{i\Phi} = \left(\frac{\delta I_{mb}}{I_{mb}}\right)^{1/2} (\cos\Phi + i\sin\Phi)$$

From there, T940063 considers only the imaginary part of the above expression. For the radiation pressure component, we consider the real part. Note that δI_{mb} is the amplitude of the field added to the main beam (at the ETM); this field will be built up by the cavity signal gain, and since we need the total cavity field to compute the radiation force, we need to include this signal gain, denoted by Γ. The intracavity field is then:

$$\psi_{mb} + \delta\psi_{mb}\Gamma = \psi_{mb}(1 + (\delta I_{mb}/I_{mb})^{1/2}\,\Gamma\cos\Phi)$$

where in the right hand side we have taken only the real part. The intracavity power is the modulus squared of this quantity, and the fluctuating part of the power is:

$$\delta P_c = 2(I_{mb}\,\delta I_{mb})^{1/2}\,\Gamma\cos\Phi$$

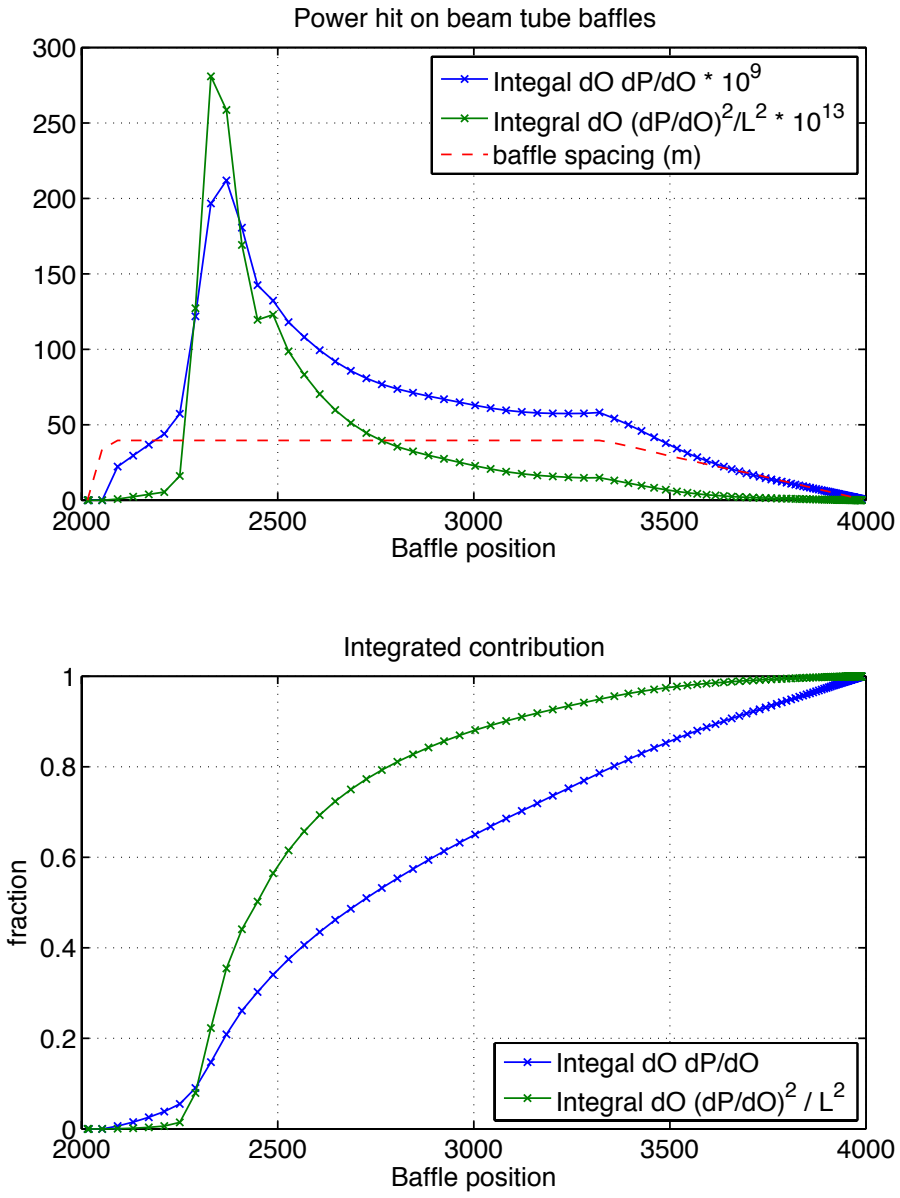

Figure 8: Scattered light power from the ETM at each beam tube baffle location (upper panel; blue points). Values are calculated with the SIS output, summing the power in all the simulation pixels for a given baffle. The green points scale these values by r^{-2} (distance from the ETM), to indicate their relative contribution to the sum in eq. 3. The lower panel gives the cumulative sum of the upper panel points (normalized).

Following the same line of reasoning as in T940063 for the phase shift Φ (section II.C), the power spectrum of the phase term is:

$$\tilde{S}^2_{\cos\Phi} = \frac{1}{2}\left(\frac{4\pi}{\lambda}\right)^2 \tilde{x}_b^2(f)$$

The power spectrum of the cavity power fluctuations is thus:

$$\delta\tilde{P}_c^2 = 2(I_{mb}\,\delta I_{mb})\,\Gamma^2\left(\frac{4\pi}{\lambda}\right)^2 \tilde{x}_b^2(f)$$

The force on *both* the ETM and the ITM is $(2\,\delta\tilde{P}_c/c)$, and the two forces are coherent: the force fluctuation pushes the test masses apart, or pulls them together, depending on the sign. The resulting cavity length fluctuation noise spectrum is thus:

$$\delta\tilde{x}_c^2(f) = \left(\frac{2}{M(2\pi f)^2}\frac{2\,\delta\tilde{P}_c}{c}\right)^2 \tag{5}$$

$$= \frac{8}{M^2(2\pi f)^4}\left(\frac{2}{c}\right)^2 (I_{mb}\,\delta I_{mb})\,\Gamma^2\left(\frac{4\pi}{\lambda}\right)^2 \tilde{x}_b^2(f)\,, \tag{6}$$

where M is the mass of the test mass (40 kg).

4.5 Cavity signal gain Γ

The field sidebands injected at the ETM see the effective reflectivity of the ITM-SRM cavity, r':

$$\begin{aligned} r_{ITM} &= \sqrt{(1-0.014)} = 0.993 \\ r_{SRM} &= \sqrt{(1-0.35)} = 0.806 \\ r' &= \frac{r_{ITM}-r_{SRM}}{1-r_{ITM}r_{SRM}} = 0.936 \end{aligned}$$

The signal field gain is then:

$$\Gamma = \frac{1}{1-r'} = 15.7$$

4.6 Comparison of phase and amplitude effects

Equation 1 of this note gives the equivalent test mass noise due to phase noise produced by scattered light, and equation 6 gives the cavity length noise due to amplitude noise produced by scattered light. The former will dominate at higher frequencies, and the latter at lower frequencies. Setting them equal gives the frequency at which the transition occurs:

$$\begin{aligned} f^2 &= \frac{8}{Mc\lambda\pi}\,\Gamma\,I_{mb} \\ f &= 48\,\mathrm{Hz}\left(\frac{I_{mb}}{750\,\mathrm{kW}}\right)^{1/2} \end{aligned}$$

4.7 Pulling it all together

Including both phase and amplitude terms, the equivalent arm cavity length fluctuation power spectrum, due to the scattering in a single arm cavity, is:

$$\delta\tilde{x}_c^2(f) = \frac{1}{2}\left(\lambda^2 + \left(\frac{8\,\Gamma I_{mb}}{cM\pi f^2}\right)^2\right)\frac{dP}{d\Omega_{bs}}\,\tilde{x}_b^2(f)\sum_i K^i\,. \tag{7}$$

The value of the sum of the K^i is given in Eq. 4 above. To account for both arm cavities we would remove the leading factor of 1/2.

Comment on scaling with amplitude of the coating ripple: the equivalent displacement noise due to this scattered light goes as $x \propto dP/d\Omega_{ms}$, and the scattering probability scales as the square of the ripple amplitude. Therefore, if we want to reduce the scattered light displacement/strain noise by a factor of X, the coating ripple amplitude must be reduced by a factor $\sqrt{X}$.

5 Beam tube motion

For the spectrum of beam tube motion, $\tilde{x}_b(f)$, we have three data sets available. One set was taken by R. Weiss in 2000, and was measured on the LHO insulated beam tube (see LIGO-T1300331). This set includes a measurement of the longitudinal beam tube acceleration (along the tube axis), taken near a tube support ring (where the baffles should be mounted). The second set of data was taken by R. Schofield at LHO in August 2007. These measurements were made with an accelerometer mounted radially on the beam tube in the LVEA, on the beam tube side of the gate valve, right by the building wall. The third set was taken by Schofield in April 2013 at LHO, at a couple of places along the beam tube. Wind speeds were high during this most recent set of measurements. Representative vibration spectra from all three sets are shown in Fig. 9. For the April 2013 data, we also show the measured vibration transverse to the tube axis; above the 13-14 Hz mode, the transverse motion is much larger than the longitudinal motion.

6 Results

Using these vibration spectra for the baffle motion, we calculate the scattered light noise in terms of equivalent displacement noise using equation 7, doubled to account for both arms. We use a baffle BRDF [2] of $dP/d\Omega_{bs} = 0.02$ str^{-1}. The results are shown in Fig. 10 and Fig. 11. Given that the transverse motion of the beam tube is much higher than the longitudinal motion above about 15 Hz, we also include in Fig. 11 a 'worst case' estimate where we do not assume that only the longitudinal motion leads to scattered light noise. For this estimate (gray curve) we make an incoherent sum of the motion in the 3 axes plotted in Fig. 9.

[2] Value from Rai Weiss, for the BRDF of the beam tube baffles as viewed from the back.

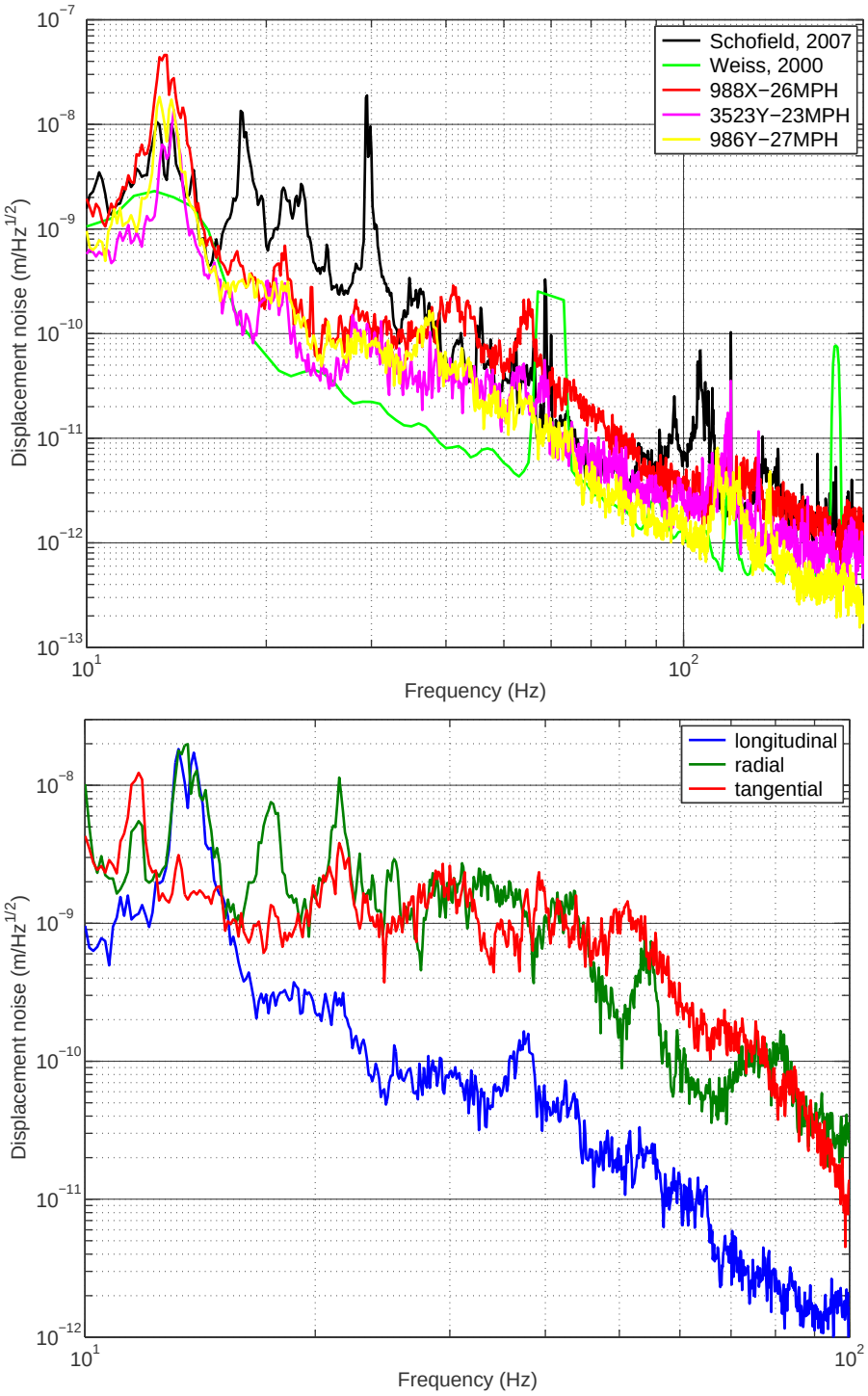

Figure 9: **Top.** Black: Vibration spectrum of the LHO Y-arm beam tube, radial direction. This is measured in the LVEA, on the beam tube side of the gate valve. Green: LHO insulated beam tube longitudinal motion, measured near a tube support ring. Red/magenta/yellow: LHO longitudinal beam tube motion, measured by Schofield, April 14, 2013. The legend for each curve indicates: distance from the beamsplitter, in meters; arm, X or Y; wind speed. These measurements were made near tube fixed supports. The 30 Hz peak seen in the Schofield 2007 data is likely due to mechanical vibration in the LVEA. **Bottom.** Data corresponding to *988X* in the top panel, and including transverse degrees-of-freedom.

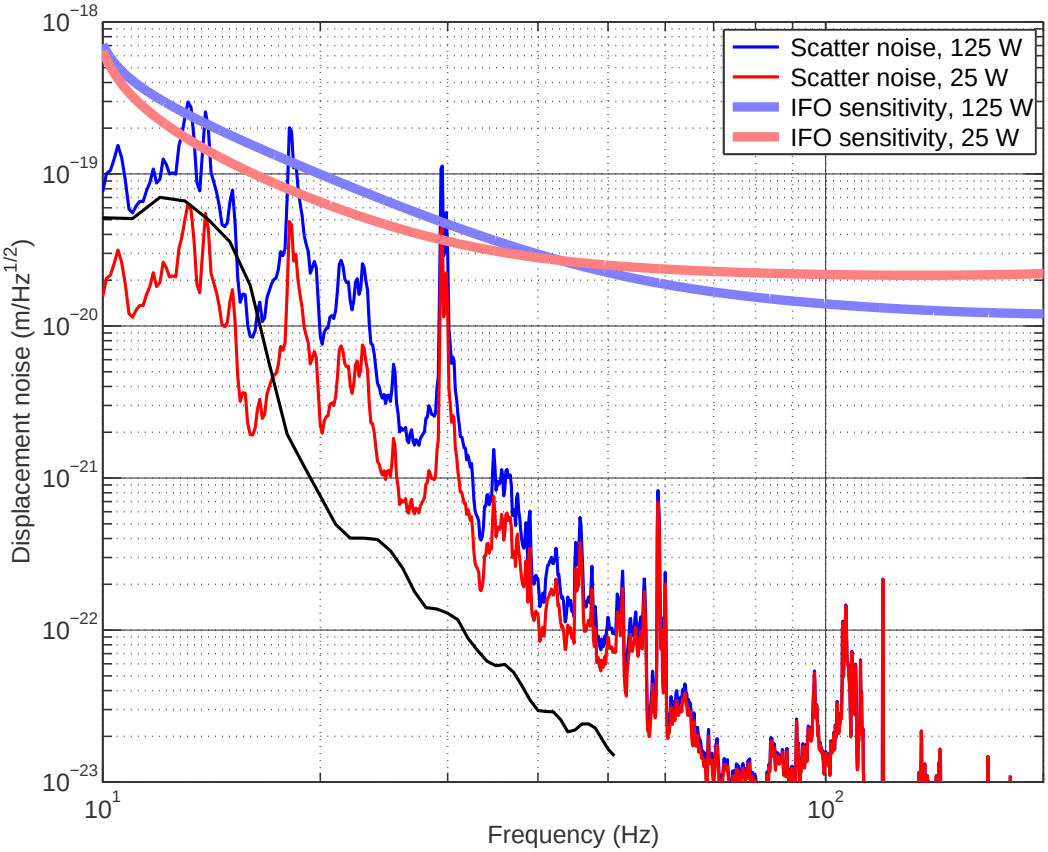

Figure 10: Displacement noise due to scattered light recombination from the beam tube baffles, along with the interferometer displacement noise as calculated by GWINC. For gravitational wave strain noise, divide all curves by 4000 m. Red/light red curves: calculated for 25 W input to the interferometer, 150 kW power in the arms. Blue/light blue curves: calculated for 125 W input to the interferometer, 750 kW power in the arms. Blue and red scatter noise curves use the Schofield 2007 beam tube vibration data; this data is probably not very representative, as it is taken in the LVEA, and is radial motion, rather than longitudinal. The **black** curve is the scattered light noise estimate using the Weiss vibration data, for the 125 W case. Other GWINC parameters: zero detuning of the signal recycling cavity; signal recycling mirror transmission of 35%.

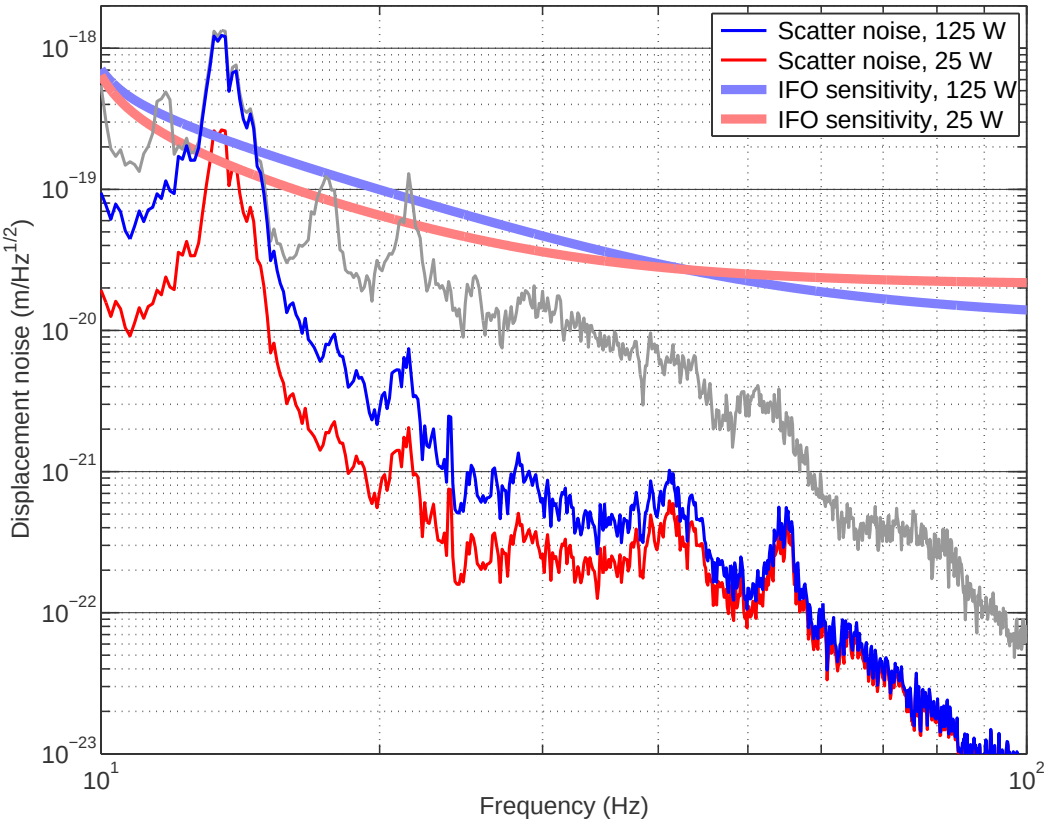

Figure 11: Displacement noise due to scattered light recombination from the beam tube baffles, along with the interferometer displacement noise as calculated by GWINC (same as in Fig. 10). For gravitational wave strain noise, divide all curves by 4000 m. Red/light red curves: calculated for 25 W input to the interferometer, 150 kW power in the arms. Blue/light blue curves: calculated for 125 W input to the interferometer, 750 kW power in the arms. Scatter noise curves use the Schofield April 2013 beam tube vibration data, in particular the **988X-26MPH** curve from Fig. 9. While this data gives the desired longitudinal motion at a representative point along the tube, the effects of the high wind speeds are unknown at this time. *Gray curve:* this is a worst case estimate, as described in the text; this uses the beam tube motion in all 3 axes shown in Fig. 9, not just the longitudinal motion.

7 Updates

Since v2 of this document (April 2013), more measurements of beam tube vibrations have been made, both at LHO and LLO. Details of these measurements can be found in the electronic log book entries–LHO: 6418; LLO: 7296, 6889, 6856. Here we just summarize the motion amplitude at the 14 Hz mode of the tube.

Location	*Condition*	*Amplitude* ($\mathrm{m}/\sqrt{\mathrm{Hz}}$)	*Rel. to strain noise*
LHO-988Y	No wind, near FS	1×10^{-8}	$1\times$
LHO-988X	30 mph wind, near FS	$4 - 5 \times 10^{-8}$	$4 - 5\times$
LHO-986Y	30 mph wind, near FS	$1.5 - 2 \times 10^{-8}$	$1.5 - 2\times$
LHO-3523Y	30 mph wind, near FS	$1 - 1.5 \times 10^{-8}$	$1 - 1.5\times$
LHO-988X	no wind, near FS	1×10^{-8}	$1\times$
LLO: Y arm, near mid	uninsulated	7×10^{-9}	$0.7\times$
LLO: X arm, near mid	insulated	$1 - 1.5 \times 10^{-9}$	$0.1 - 0.15\times$
LLO: Y arm, 250m from mid	insulated	3×10^{-9}	$0.3\times$

Table 1: Amplitude of beam tube motion, along the beam tube axis, at the 14 Hz mode. FS: fixed support; other designations are as given above. The last column indicates the strain noise produced by this motion, calculated using equation 7, relative to the interferometer design strain noise for high power (125 W input) operation. Ideally, the factors in this column would be 0.1 or smaller.

All of the LHO measurements in the above table were made on insulated beam tube sections. Later measurements at LHO on an uninsulated section showed that the 14 Hz mode is affected very little by the insulation, though it does provide significant damping above about 50 Hz.

The other new information is that Richard Day used the FOG FFT simulation tool to simulate the scattering process to and from a beam tube baffle, comparing the simulation results with the analytical formulation used here (section 4.1); see LIGO-G1300532 for details. Day performed 10,000 simulations, randomizing the baffle surface for each, yielding a distribution of coupling factors (coupling of scattered light back into the cavity mode). The most probable coupling factor was in fact equal to the analytic factor used here (65% of the coupling factors were at or below the analytic value). At the 90% probability level, the coupling factor was about $2\times$ higher than the analytic value. The scattered light strain noise goes as the square root of this coupling factor. The simulation results suggest that a more conservative estimate of the scattered light noise would be $1.5 - 2\times$ higher than the values given above that use the analytic expression.